TOWARDS A COMPREHENSIVE SEISMIC VELOCITY MODEL FOR THE BROADER AFRICA-EURASIA COLLISION REGION, TO IMPROVE NUCLEAR EXPLOSION MONITORING

S. van der Lee[1], A. Rodgers[2], M. Flanagan[2], M. Pasyanos[2], F. Marone[3], and B. Romanowicz[3]

Northwestern University[1], Lawrence Livermore National Laboratory[2], and UC Berkeley[3]

Sponsored by National Nuclear Security Administration
Office of Nonproliferation Research and Engineering
Office of Defense Nuclear Nonproliferation

Contract Nos. DE-FC52-04NA25541[1], W-7405-ENG-48[2], and DE-FC52-04NA25542[3]

ABSTRACT

We report on progress towards a new, comprehensive three-dimensional (3-D) model of seismic velocity in a broad region encompassing the Middle East, northern Africa, the Mediterranean Sea, the Levant, the Arabian Peninsula, the Turkish-Iranian Plateau, the Indus Valley, and the Hindu Kush. Our model will be based on regional waveform fits, surface wave group velocity measurements, teleseismic arrival times of S and P waves, receiver functions, and published results from active source experiments. We are in the process of assembling each of these data sets and testing the joint inversion for subsets of the data. Seismograms come from a variety of permanent and temporary seismic stations in the region. Some of the data is easily accessible through, for example, IRIS, while collection of other data is more involved. This work builds on ongoing work by Schmid et al. (2004, and manuscript in preparation).

In these proceedings, we highlight our data sets and their inferences, demonstrate the proposed new data-inversion modeling methodology, discuss results from preliminary inversions of subsets of the data, and demonstrate the prediction of arrival times with three-dimensional velocity models. We compare our preliminary inversion results with the results of Schmid et al., and the predicted arrival times to ground-truth data from the National Nuclear Security Administration (NNSA) Knowledge Base. Our data sets are simultaneously redundant and highly complementary. The combined data coverage will ensure that our three-dimensional model comprises the crust, the upper mantle, including the transition zone, and the top of the lower mantle, with spatially varying, but useful resolution.

The region of interest is one of the most structurally heterogeneous in the world. Continental collision, rifting and sea-floor spreading, back-arc spreading, oceanic subduction, rotating micro plates, continental shelf, and stable platforms, are just some of the region's characteristics. Seismicity and the distribution of seismic stations are also geographically heterogeneous. The crustal thickness ranges from near 20 to near 45 km under dry places in the Mediterranean region alone, which contains at least seven of the fourteen types of crust defined globally by Mooney et al. (1998). The S-velocity varies laterally by an entire 1 km/s over 1000 km within the uppermost mantle. On average the S-velocity is 50 to 150 m/s slower, between a depth of 150 km and the Moho, than global model IASPEI91. These lowered S velocities reflect the high amount of tectonic activity in the study region. In the transition zone,the S-velocity is roughly 150 m/s higher than IASPEI91. These heightened S velocities likely reflect the numerous fragments of oceanic lithosphere that subducted in the study region during geologically relatively recent times.

OBJECTIVES

Our primary objective is developing a new 3-D S-velocity model for the Middle East and Mediterranean region, including North Africa, southern Europe, and Arabia that

1) is resolved in aseismic regions,
2) is resolved throughout the upper mantle (to 660 km),
3) resolves laterally varying crustal thickness,
4) contains laterally varying vertical velocity gradients,
5) is simultaneously compatible with multiple data sets,
6) utilizes several recent, unique waveform data sets,
7) includes uncertainties of the model parameters.

These features would increase the model's ability to predict and calibrate regional travel times and waveforms, thereby providing improved event locations, focal mechanisms, and other event discriminants.

Secondly, we aim to convert the 3-D *S*-velocity model to a 3-D *P*-velocity model, using both literature on elastic properties (and their partial derivatives with temperature and pressure) of mantle rocks and empirical information provided by measured arrival times of teleseismic *P* and *P*ms waves. The corresponding *P*-wave model would provide an improved ability to locate seismic events.

The prediction and calibration of regional travel times and waveforms depends strongly on the methodology used to compute travel times and waveforms. Our third objective is to test the *S*-wave and *P*-wave models' ability to predict regional *P* and *S* travel times, deflect wave paths, and deform waveforms, and assess their effects first on the studied seismograms (travel times and waveforms) and subsequently on the 3-D models derived from these data.

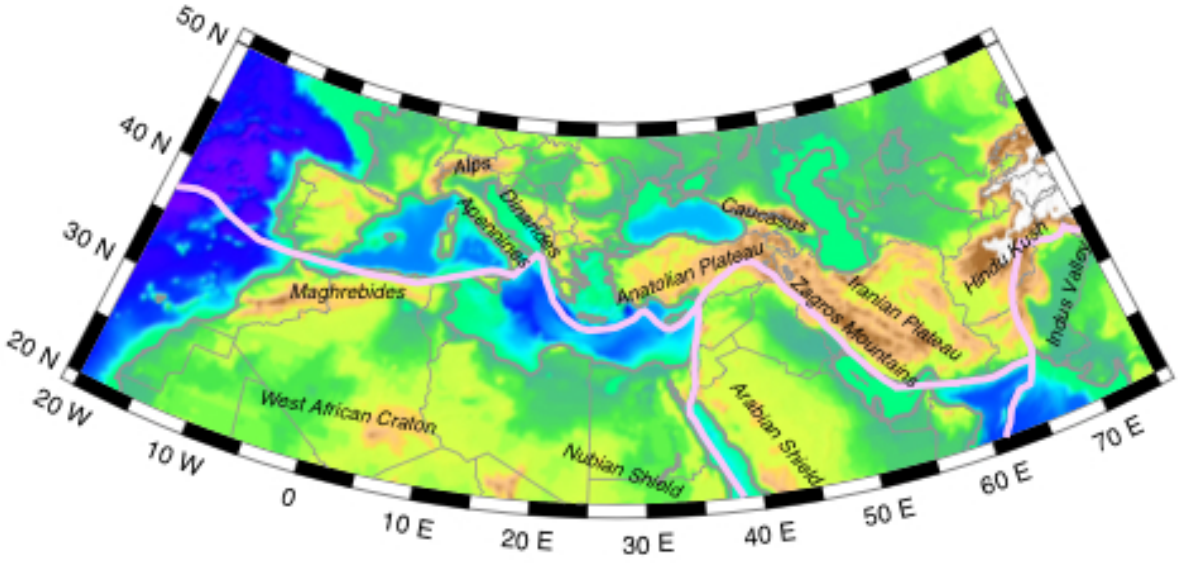

Figure 1. Topographic map of the study region. The pink line is the NUVEL1-A (DeMets et al., 1990) representation of the Eurasia-Africa-Arabia plate boundary.

The study region (Figure 1) is roughly centered around the Africa-Arabia-Eurasia triple junction. Two other triple junctions mark the western and eastern boundaries of the study region, with the Africa-Eurasia-North America junction at the Azores being just off the map in the west and the Arabia-Eurasia-Indian Plate junction at the edge of the study region to the east (Figure 1). The interaction of these six major tectonic plates with each other and with several microplates within a stretch as short as one quarter of the Earth's circumference makes this study region tectonically complex. The 3-D structure of the upper mantle and crust are correspondingly complex. More than half of the primary crustal types used by Mooney et al. (1998) for the construction of their global crustal model

CRUST5.1 are found in the study region. In many parts of the region the seismic *S*-velocity of the upper mantle strongly varies laterally and by large amounts (e.g. Pasyanos et al., 2001; Marone et al., 2004; Maggi and Priestley, 2005). We plan to capture various renditions of this structurally and tectonically complex part of the world in one model through the joint inversion of different types of seismic data. Predictions for seismogram characteristics (phase arrival times, amplitudes, dispersion) based on this new model are expected to match many of the observed characteristics and be useful for event discrimination. Simultaneously, the new model will refine our understanding of the structure and tectonics in the study region.

RESEARCH ACCOMPLISHED

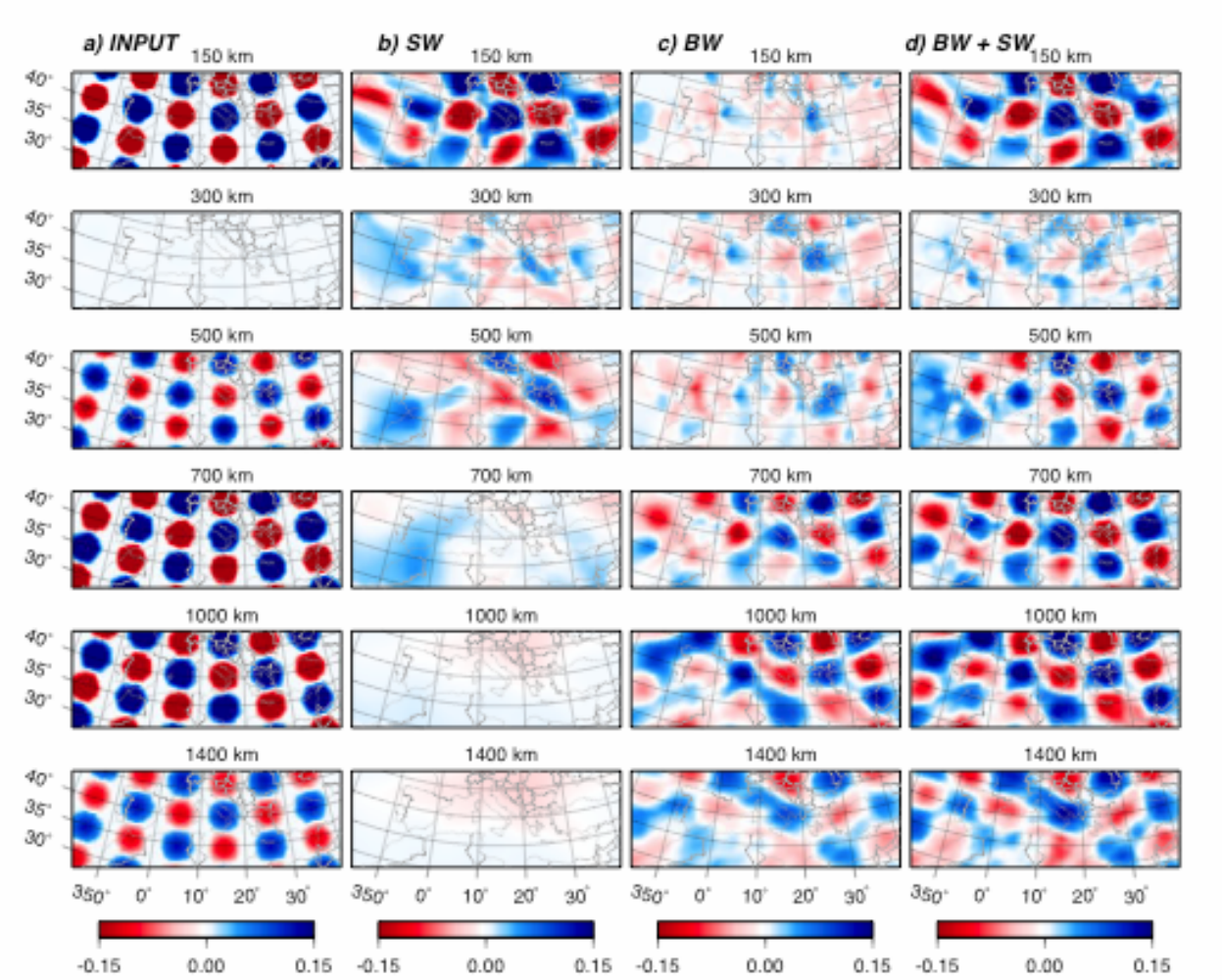

Figure 2. Joint-inversion resolution test for the western part of the study region. INPUT = hypothetical model, SW = resolved with regional waveforms only, BW = resolved with teleseismic *S* arrival times only, BW + SW = resolved by the joint inversion of both data sets.

Joint inversion

To achieve our primary objectives we are developing software than handles the joint inversion of constraints from regional waveform fits, teleseismic arrival times, receiver functions, and group velocities. We have completed the software for jointly inverting regional waveforms, receiver functions, and teleseismic arrival times. The joint inversion code has been tested on the teleseismic *S* arrival time data set of Schmid et al. (2004) and the data derived from regional waveform fitting from Marone et al. (2004). The results are encouraging, showing only a percent or two increase in the variance reduction obtained in the linear inversion of both data sets compared to their individual

inversions (Schmid et al., manuscript in preparation). The resolving power of the joint data sets, however, has increased dramatically (Figure 2). Figure 2 demonstrates the following: The teleseismic data add more lateral resolution to the regional waveform data, while the regional waveform data add more depth resolution to the teleseismic data. The resolved depth range of the combined data sets has doubled with respect to their individual depth ranges. The regional waveform data resolve the upper mantle more strongly while the teleseismic arrival times resolve the lower mantle more strongly. Where the two data sets overlap in spatial sensitivity, e.g.,in the transition zone (see the 500-km map in Figure 2), the resolving power of the combined data is superior to that of each of the data sets alone.

Example Waveform Fits

We have begun to fit the available waveform data in the Middle East using the non-linear inversion procedure employed by previous partitioned waveform inversion studies (Van der Lee and Nolet, 1997; Marone et al. 2004). Figure 3a shows the Middle East region and four events and paths for which we have estimated path-average structure. Earthquakes are indicated by their Harvard centroid moment tensor (CMT) solutions. These four paths sample some of the diversity of geologic/tectonic environments in the Middle East (Figure 1). The velocity structures were estimated using the average continental model MC35 (Van der Lee and Nolet, 1997), shown as the black line in Figure 3b, however we chose an appropriate crustal thickness for each path (in 5-km increments) based on a priori reported estimates. The inversion procedure estimates the perturbations to the starting model by non-linear optimization (Nolet et al.;1986; Nolet, 1990).

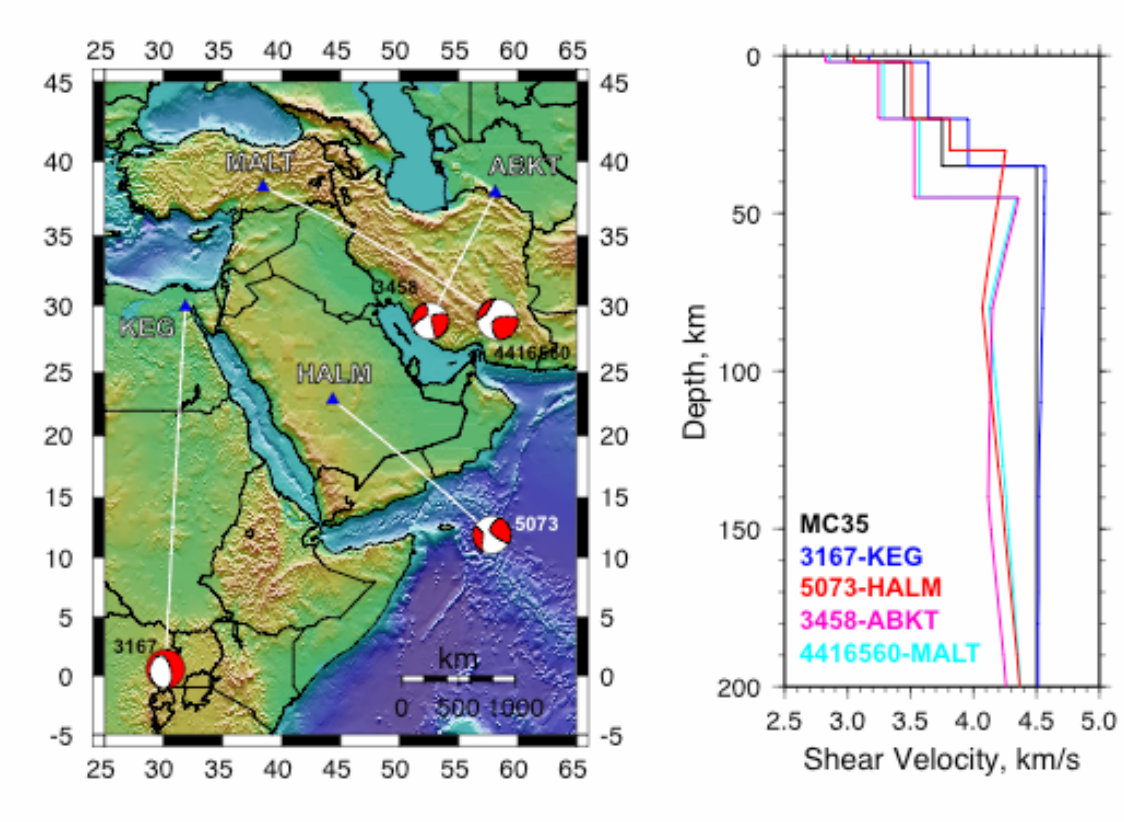

Figure 3. (a) Map of the Middle East showing four earthquakes and paths for which we fit waveforms. The events are indicated by their moment tensor and identified by their eventid (evid) number. Stations are shown as blue triangles. (b) Shear velocity profiles for the four paths shown in (a), color-coded by path (indicated by evid-station). The starting model, MC35, is shown in black.

The resulting shear-velocity profiles for these paths are shown in Figure 3b. These models show 1) faster crustal velocities and slightly faster mantle velocities for the Nubian shield (KEG); 2) lower velocities in the crust and upper mantle for the path crossing the Iranian Plateau (ABKT and MALT); faster crustal and low sub-Moho velocities path from the Owen Fracture Zone to the Arabian Shield (HALM). We discuss the fits and interpret the inferred structures in detail below.

The waveform fits are shown in Figure 4. These panels show the data (black) and synthetic seismograms for the starting model (red dashed) and final model (green). The starting model often predicts significant phase differences relative to the data for both the S- and Rayleigh waves. The path across the Nubian Shield (3167-KEG) is faster than the MC35 starting model. The crustal velocities along this path are quite high. This is consistent with fast crustal velocities in the Arabian Shield (e.g., Mokhtar and Al-Saeed, 1994; Sandvol et al., 1998; Rodgers et al., 1999; Julia et al., 2003; Al-Damegh et al., 2005). It is worth noting that the Red Sea broke up the Nubian-Arabian Shield and these provinces could have similar crustal petrologies. Both provinces have volcanics and it has been speculated that mafic intrusion may explain the higher crustal velocities. The inferred mantle velocities beneath the Nubian Shield are slightly faster than the starting model. However, reported mantle velocities beneath the Arabian Shield are lower than average (e.g., Mokhtar and Al-Saeed, 1994; Rodgers et al., 1999, Maggi and Priestley, 2005). Constraints on mantle velocities beneath the Nubian Shield will improve understanding of mantle dynamics associated with the opening of the Red Sea, including possible asymmetries across the axis of rifting.

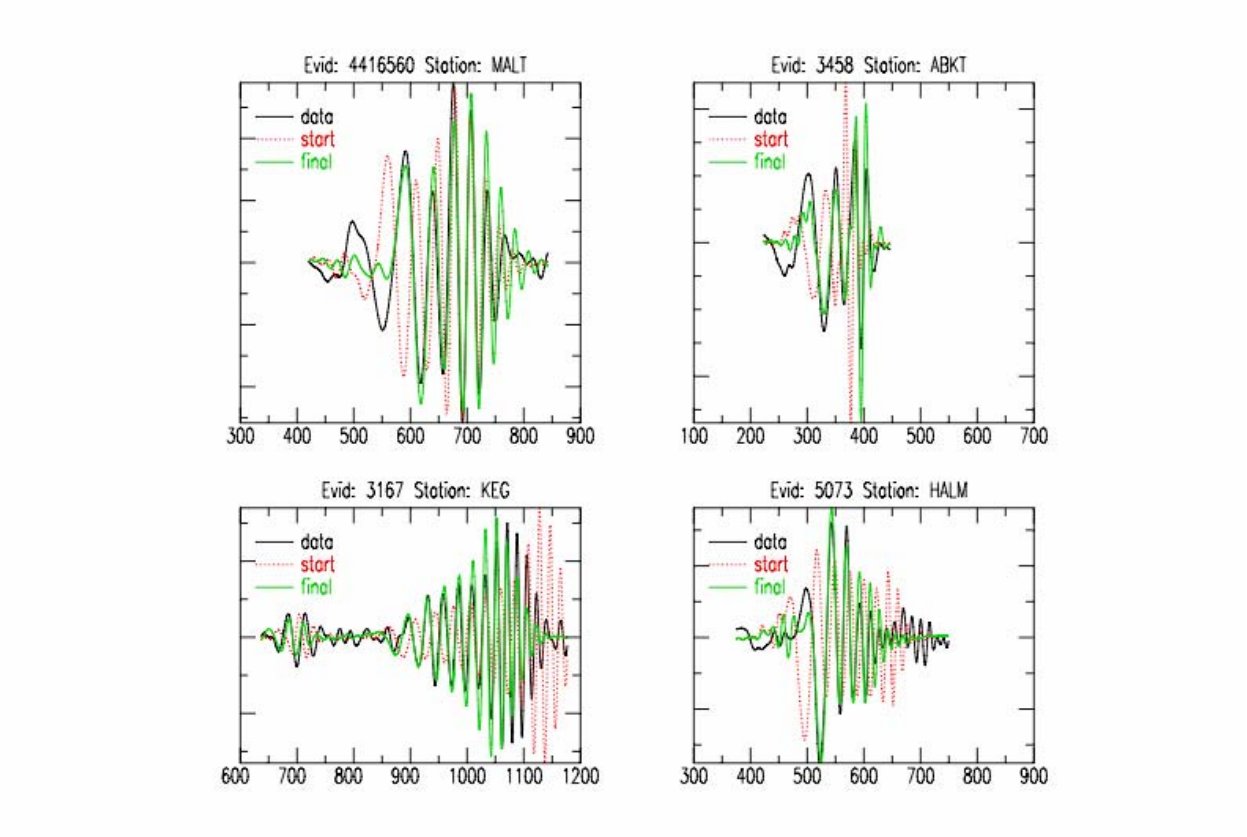

Figure 4. Fits for vertical component S- and Rayleigh waveforms for the four paths: (a) 4416560-MALT; (b) 3458-ABKT; (c) 3167-GNI; and (d) 5073-HALM. The waveforms are shown as observed (black), starting model (red dashed) and final (green). The frequency content of the data and synthetics is different for each fit but generally covers the band 0.006-0.04 Hz

The paths across the Iranian Plateau (3458-ABKT and 4416560-MALT) are fit with a model with 45-km crust, consistent with estimates of crustal structure in the Zagros Mountains (Hatzfeld et al., 2003). Estimated crustal

velocities in the Iranian Plateau are low, consistent with an orogenic crust. Mantle velocities beneath the Iranian Plateau are low, consistent with previous reports (e.g., Hearn and Ni, 1994; Al-Lazki et al., 2004; Maggi and Priestley, 2005). Note that this is a zone of high Sn attenuation, likely related to partial melt and shallow asthenospheric mantle (e.g., Kandinsky-Cade et al., 1981; Rodgers et al, 1997; Al-Damegh et al., 2004). The waveform fits for these paths are satisfactory for the Rayleigh wave, but the S-wave and higher-mode Rayleigh wave are not particularly well fit. This could result from Love wave energy that scattered onto the vertical component for the 4416560 (Dec. 26, 2003 Bam Iran) event. The radiation pattern for this event is nearly nodal for Rayleigh waves and thus maximal for Love waves. The long-period energy preceding the Rayleigh wave could be a quasi-Love wave due to anisotropy or multi-pathing.

The path from the Owen Fracture Zone to the Arabian Shield (5973-HALM) reveals low mantle velocities. This mixed oceanic-continental path was fit with a model with intermediate crustal thickness of 25 km. Mantle velocities are low, but this is not surprising given that the path passes through oceanic spreading centers along the Owen Fracture Zone and across the Gulf of Aden.

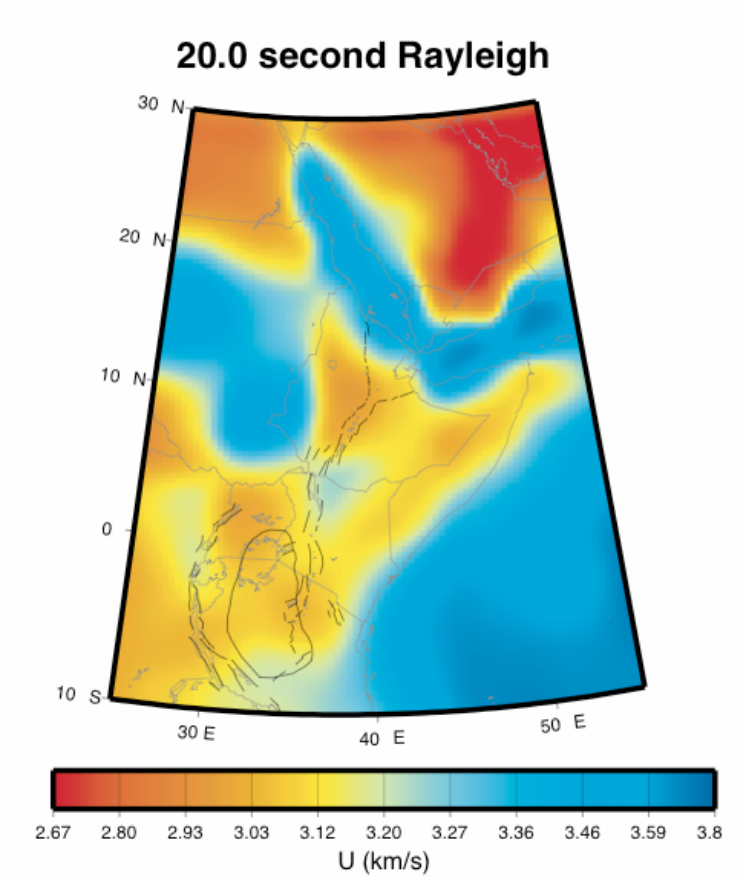

Figure 5. Inferred spatial variation in group velocity (U) for 20s Rayleigh waves.

Rayleigh group velocities

We have continued to measure group velocities of Rayleigh waves and use them to update previous group velocity maps (Figure 5). Twenty second Rayleigh waves are very sensitive to the crust, which is reflected in the stark group velocity contrast between the oceanic (and Red Sea) regions and the slower continental regions, with thicker crust (Figure 5). Pinpointing the cause of the group velocity differences within continental regions (Figure 5) awaits the analysis of the depth distribution of the *S*-velocity anomalies that give rise to the anomalous group velocities. The contrast between the Nubian Shield and Arabian peninsula in Figure 5 is, however, qualitatively consistent with the waveform fits (Figure 4) and their constraints on upper mantle structure (Figure 3), which show relatively high

velocity in the uppermost mantle between event 3167 and station KEG and relatively low velocities between event 5073 and station HALM. This consistency supports the anticipated benefits of a joint inversion.

Surface-wave group velocities can be reliably measured without knowledge of the event source mechanism. An important new source in the study region of data for such group velocity measurements is the MIDSEA data set (Van der Lee et al., 2001). Surface waves in the MIDSEA data have been analyzed for those events for which source mechanisms were available, but not yet for others.

Data transcription and conversion

The MIDSEA data are from a temporary PASSCAL-type experiment with an unusual mix of instrumentation and data formats. Conversion to a community-accepted exchangeable and complete data format (SEED) facilitates their analysis in a broader sense and into the future. A station list (Table 1) hints at the heterogeneity among stations and the data-processing procedures associated with each (Van der Lee et al., 2001). While data from some stations are already available in full SEED format at the IRIS or Geofon data centers, others lack continuity of records and/or response information, precluding them from conversion to SEED and the associated storage in a long-term accessible archive. We have transcribed and submitted the remainder of the MIDSEA data to the IRIS data management center (DMC) storage facilities and have assembled and tested a procedure to reliably convert the data to SEED format.

The quality of MIDSEA data is also heterogeneous. For some station location choices, environments that provided more security prevailed over environments providing better seismic recording ability. Many of the stations required 220 V AC, restricting the locations to existing facilities. None of the stations were telemetered, resulting in significantly delayed detection of normal problems with a station. The far and remote locations of the stations, relative to the project's headquarters, as well as international customs regulations and a limited budget, caused further delays in station repair in some cases. Some have been converted to permanent station sites. For example, stations MELI, GHAR, and MARJ are now permanent Geofon and CLTB is now a MedNet station.

Table 1. MIDSEA station information. COSEA stations, installed in the Azores (Van der Lee et al., 2001; Silveira et al., 2002), are excluded in this table. COSEA data are available at the IRIS DMC. MIDSEA station names are FDSN approved. * = station was moved a few 100 m

Station code	Latitude	Longitude	Elevation (m)	Approximate on date (dd.mm.yyyy)	Approximate off date (dd.mm.yyyy)	Data location and contact
CDLV	29.163	-13.444	37	07.06.1999	06.04.2001	IRIS, Van der Lee & Cabildo de Lanzarote
EBRE	40.823	0.494	36	17.06.1999	13.11.2000	IRIS, Van der Lee & Observatori de l'Ebre
POBL	41.379	1.085	550	14.11.2000	31.03.2003	University of Barcelona, Van der Lee & LEGEF
DUOK	44.113	14.932	115	16.07.1999	05.02.2001	IRIS, Van der Lee & University of Zagreb
HVAR	43.178	16.449	250	13.10.1999	08.02.2001	IRIS, Van der Lee & University of Zagreb
ITHO	37.179	21.925	400	23.10.1999	15.08.2001	IRIS, Van der Lee & NOA
KOUM	37.704	26.838	340	28.10.1999	15.08.2001	IRIS, Van der Lee & NOA
APER	35.55	27.174	250	03.11.1999	15.08.2001	IRIS, Van der Lee & NOA

Station code	Latitude	Longitude	Elevation (m)	Approximate on date (dd.mm.yyyy)	Approximate off date (dd.mm.yyyy)	Data location and contact
MELI	35.290	-2.939	41	17.12.1999	21.11.2001	Geofon, Van der Lee & ROA
GHAR	32.122	13.089	650	19.01.2000	10.11.2002	IRIS, Van der Lee & LCRSSS
MARJ	32.523	20.878	300	22.05.2000	17.10.2001	IRIS, Van der Lee & LCRSSS
ABSA	36.277	7.473	1025	18.07.2000	03.04.2002	IRIS, Van der Lee & CRAAG
CLTB	37.579	13.216	955	01.06.1999	30.09.2000	ORFEUS, Margheriti & INGV
SALI	38.564	14.833	360	01.06.1999	30.09.2000	ORFEUS, Margheriti & INGV
VENT	40.795	13.422	110	01.06.1999	30.09.2000	ORFEUS, Margheriti & INGV
DGI	40.318	9.607	343	29.07.1999	30.06.2000	University of Nice, Deschamps
GRI	38.822	16.420	525	15.07.1999	30.06.2000	University of Nice, Deschamps
MGR	40.138	15.554	297	14.07.1999	31.03.2001	University of Nice, Deschamps
SOI	38.073	16.055	300	15.07.1999	31.03.2001	University of Nice, Deschamps

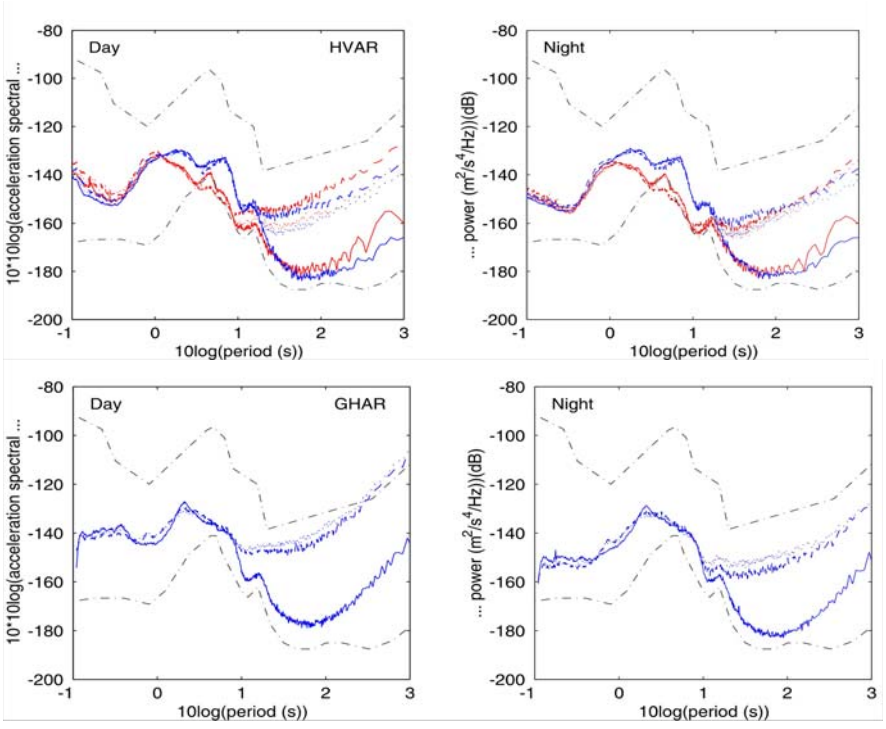

Figure 6. Acceleration spectral density of time series at two MIDSEA stations. Red and blue lines represent summer and winter, respectively. Solid and non-solid represent vertical and horizontal components, respectively. Grey dashed lines represent the Peterson high and low noise models. Earthquake records have not been removed from the time series.

Heterogeneity in MIDSEA data quality is illustrated in Figure 6. The spectral characteristics for two stations are extreme in that they both extend the Peterson noise model. The winter spectra for the horizontal components of station GHAR exceed the high noise model at the longest periods. The absence of this extreme during the night suggests that this might have something to do with human usage of the facility and its immediate environment that houses the seismometer. This seismometer was later moved to a vault. The summer spectra for HVAR are slightly below the low noise Peterson model at periods of several seconds. This illustrates the exclusiveness of the Hvar, Croatia, astronomical observatory that houses the station. Other time series spectra (not shown) demonstrate, among other issues, that the microseismic noise level is much higher in the Atlantic Ocean than in the Aegean Sea.

CONCLUSIONS AND RECOMMENDATIONS

The strength of a joint inversion of different types of seismic data lies in the various data sets being both redundant and complementary. The redundancy is needed to increase accuracy and to ensure that both data sets measure the same structural phenomena. The data sets need to be complementary to increase resolving power over a larger volume of mantle and crust and thereby reduce trade-offs, e.g.. between crustal thickness and uppermost mantle velocity, inherent in each type of seismic data set.

The broad consistency between seismic velocity anomalies inferred from teleseismic arrival times, Rayleigh wave group velocities, and regional waveforms shown here implies that these different types of data sets are at least in part redundant. The consistency further shows that the data sets record the same structural phenomena, despite differences in size and character between typical sensitivity kernels for each data set. This conclusion is further supported by an analysis of how teleseismic delay times depend on frequency (Schmid et al., 2004).

We have also shown that the teleseismic arrival times and the regional waveforms are highly complementary. The shared sensitivity, though different in character, of receiver functions and Rayleigh wave group velocities to crustal structure is anticipated to separate crustal effects on the observed data from mantle causes when included in the joint inversion.

Preliminary results from data analysis for the Middle East show that this part of the study region is slower on average than typical one-dimensional global velocity models. Marone et al. (2004) and Maggi and Priestley (2005) show that the same is true for the parts of the study region to the west and east, respectively. This allows for a fairly simple set of one-dimensional starting models, yielding a more uniform treatment of data recorded throughout the region. Our data analysis results are broadly consistent with results from the literature.

ACKNOWLEDGEMENTS

Christian Schmid produced Figure 2. Rick Benson helped with the conversion of the MIDSEA data to SEED format.

REFERENCES

Al-Damegh, K., E. Sandvol, A. Al-Lazki, and M. Barazangi (2004), Regional wave propagation (Sn and Lg) and Pn attenuation in the Arabian plate and surrounding regions, *Geophys. J. Int*. 157: 775–795.

Al-Damegh, K., E. Sandvol, and M. Barazangi (2005), Crustal structure of the Arabian plate: New constraints from the analysis of teleseismic receiver functions, *Earth. Planet. Sci. Lett*. 231: 177–196.

Al-Lazki, A., E. Sandvol, D. Seber, M. Barazangi, N. Turkelli, and R. Mohamad (2004), Pm tomographic imaging of mantle lid velocity and anisotropy at the junction of the Arabian, Eurasian and African plates, *Geophys. J. Int*. 158: 1024–1040.

DeMets, C., R. G. Gordon, D. F. Argus, and S. Stein (1990), Current plate motions, *Geophys. J. Int*. 101: 425–478.

Hearn, T., and J. Ni (1994). Pn velocities beneath continental collision zones: the Turkish-Iranian Plateau, Geophys. J. Int., 117: 273-283.

Julia, J., C. Ammon and R. Herrmann (2003). Lithospheric structure of the Arabian Shield from the joint inversion of receiver functions and surface wave group velocities, Tectonophysics, 371: 1-21.

Kadinsky-Cade, K., M. Barazangi, J. Oliver and B. Issacs (1981). Lateral variation in high-frequency seismic wave propagation at regional distances across the Turkish and Iranian plateaus, J. geophys. Res., 86: 9377-9396.

Hatzfeld, D., M. Tartar, K. Priestley and M. Ghafory-Astiany, Seismological constraints on the crustal structure beneath the Zagros Mountain belt (Iran), Geophys. J. Int., 155: 403-410.

Maggi, A. and K. Priestley (2005). Surface waveform tomography of the Turkish-Iranian Plateau, Geophys. J. Int., 160: 1068-1080.

Marone, F., S. van der Lee, and D. Giardini (2004), 3-D upper mantle *S*-velocity model for the Eurasia-Africa plate boundary region, Geophys. J. Int., 158: 109-130.

Mokhtar, T. and M. Al-Saeed (1994), Shear wave velocity structures of the Arabian Peninsula, Tectonophysics, 230: 105-125.

Mooney, W., G. Laske, and G. Masters (1998), CRUST5.1: a global crustal model at 5 x 5 degrees, J. Geophys. Res., 103: 727-747.

Pasyanos, M.E., W.R. Walter, and S.E. Hazler (2001), A surface wave dispersion study of the Middle East and North Africa for monitoring the Comprehensive Nuclear-Test-Ban Treaty, Pure appl. geophys., 158: 1445-1474.

Rodgers, A., J. Ni and T. Hearn (1997), Propagation characteristics of short-period Sn and Lg in the Middle East, Bull. Seism. Soc. Am., 87: 396-413.

Rodgers, A., W. Walter, R. Mellors, A. M. S. Al-Amri and Y. S. Zhang (1999), Lithospheric structure of the Arabian Shield and Platform from complete regional waveform modeling and surface wave group velocities, Geophys. J. Int., 138: 871-878.

Schmid, C., S. van der Lee, and D. Giardini (2004), Delay times and shear-wave splitting in the Mediterranean region, Geophys. J. Int., 159:275-290.

Silveira, G., S. Van der Lee, E. Stutzmann, L. Matias, D. James, P. Burkett, M. Miranda, L.M. Victor, J.L. Gaspar, L. Senos, S. Solomon, J.P. Montagner, and D. Giardini (2002), Coordinated seismic experiment in the Azores, ORFEUS Newsletter, 4: 10.

Sandvol, E., D. Seber, M. Barazangi, F. Vernon, R. Mellors, and A. Al-Amri (1998), Lithospheric seismic velocity discontinuities beneath the Arabian Shield, Geophys. Res. Lett., 25: 2873-2876.

Van der Lee, S., and G. Nolet (1997), Upper-mantle S-velocity structure of North America, J. Geophys. Res., 102:22,815-22,838.

Van der Lee, S., F. Marone, M. van der Meijde, D. Giardini, A. Deschamps, L. Margheriti, P. Burkett, S.C. Solomon, P.M. Alves, M. Chouliaras, A. Eshwehdi, A.S. Suleiman, H. Gashut, M. Herak, R. Ortiz, J.M. Davila, A. Ugalde, J. Vila, K. Yelles (2001), Eurasia-Africa Plate Boundary Region Yields New Seismographic Data, Eos Trans. AGU, 82: 637 645 646.